Oxidative stress impairs the Nur77-SIRT1 axis resulting in a decline in organism homeostasis during aging

Yang Yu
Institute of Health Sciences, China Medical University
Xiaoyu Song
Institute of Health Sciences, China Medical University
Guojing Ma
Institute of Health Sciences, China Medical University
Lixia Zheng
Institute of Health Sciences, China Medical University
Xiaoxun Wang
Institute of Health Sciences, China Medical University
Feng Chen
Department of Gerontology, Shengjing Hospital of China Medical University
Tingting Liu
Department of Gerontology, Shengjing Hospital of China Medical University
Huanlian Tian
Department of Gerontology, Shengjing Hospital of China Medical University
Yingxi Xu
Institute of Health Sciences, China Medical University
Danni Li
Institute of Health Sciences, China Medical University
Fan Yang
Institute of Health Sciences, China Medical University
Liu Cao (lcao@cmu.edu.cn)
Institute of Health Sciences, China Medical University https://orcid.org/0000-0001-6471-1993
Difei Wang
Department of Gerontology, Shengjing Hospital of China Medical University

Letter

Keywords: aging, SIRT1, oxidative stress, Nur77, proteasome degradation

Posted Date: August 23rd, 2021

DOI: https://doi.org/10.21203/rs.3.rs-828701/v1

Abstract

Sirtuin 1 (SIRT1) is an NAD^+-dependent deacetylase that protects against premature aging and cellular senescence. Aging that is accompanied by oxidative stress leads to a decrease in SIRT1 level and activity, but the regulatory mechanism that connects these events has remained unclear. Here we report that Nur77, an orphan nuclear receptor that shares similar biological pathways with SIRT1, also decreases with age in multiple organs. Our *in vivo* and *in vitro* studies revealed that Nur77 and SIRT1 decrease during aging and oxidative stress-induced cellular senescence. Deletion of Nur77 shortens lifespan and accelerates the aging process in multiple mouse tissues. Overexpression of Nur77 protects SIRT1 protein from proteasome degradation through negative transcriptional regulation of the E3 ligase murine double minute 2 (MDM2). Our results show that Nur77 deficiency remarkably aggravates aging related nephropathy, and elucidate a key role for Nur77 in the stabilization of SIRT1 homeostasis during renal aging. We propose a model wherein reduction of Nur77 upon oxidative stress promotes SIRT1 protein degradation through MDM2, which triggers cellular senescence. This creates additional oxidative stress and provides positive feedback for premature aging by further decreasing Nur77 expression. Our findings reveal the mechanism of oxidative stress-reduced SIRT1 during aging and offer an attractive therapeutic strategy for targeting aging organism homeostasis.

Introduction

Aging is a biological phenomenon in which the structure and function of organisms declines with increasing age[1]. The Sir2 protein and its homologs belong to the Sirtuin family of protein deacetylases that are collectively known to extend lifespan in diverse species[2]. Of all the Sirtuins, SIRT1 is the most extensively studied member. SIRT1 deacetylates key histone residues of multiple protein targets including p53, FOXO1/3, PGC-1α, and NF-κB[3–6]. By affecting transcriptional activation, SIRT1 is involved in the regulation of a broad range of vital aging-related biological pathways, including DNA repair and apoptosis, cell stress responses, and glucose and insulin homeostasis[7–9]. SIRT1 declines with age, which disrupts the homeostasis of multiple organs and accelerates the aging process[10]. However, the driving factor for the reduction in SIRT1 during aging in mammalian systems has remained unclear.

Another factor that shows an intrinsic relationship with aging rate is the overproduction of reactive oxygen species (ROS)[11]. During the aging process, multiple age-related organ dysfunctions are associated with ROS accumulation. High levels of ROS hamper the repair of damaged nuclear and mitochondrial DNA at multiple steps and contribute to genomic instability[12–14]. SIRT1 deacetylase is associated with anti-aging effects and acts as an antioxidant by acting on epigenetic modifications[15, 16]. During the aging process, both the elevation of oxidative stress and reduction of SIRT protein have been shown to occur in senescent cells. It is likely that increasing oxidative stress during aging may be responsible for the decreasing SIRT1 level and activity.

The orphan nuclear receptor, Nur77 (also called TR3), is implicated in similar biological pathways involved in aging. Nur77 belongs to the NR4A subgroup of nuclear hormone receptors and has emerged as an important regulator of the inflammatory response, as well as of metabolic homeostasis and oxidative stress[17–19]. In macrophages, Nur77 helps repress transcription of pro-inflammatory factors, leading to a systemic decreased inflammatory response in elderly mice[20]. The overexpression of Nur77 in melanoma cells eliminates ROS accumulation by promoting fatty acid oxidation to increase NADPH and ATP levels[19]. Exactly how Nur77 connects with other pathways and molecular mechanisms involved in aging is not understood.

Here we investigated the internal regulatory mechanism that links increasing ROS levels and decreasing SIRT1 protein homeostasis during aging. We found that ROS drives Nur77 decline during aging, which leads to loss of SIRT1 via MDM2-mediated proteasome degradation. These events all help to increase p53 stability and activation, cellular senescence and ROS accumulation, which in turn further downregulate the expression of Nur77 and SIRT1 and accelerate the aging process.

Results

To search for a common regulatory mechanism that functions in multiple organs during aging, we examined differentially expressed genes in three different naturally aged tissues from NCBI GEO DataSets. We detected 461 co-regulatory genes, which were identified as significantly enriched in cell cycle process (GO:0010564), regulation of cell death (GO:0010942) and stem cell proliferation (GO:0072091) (Fig. 1a-c). Two genes were identified from the intersection of differentially expressed genes in the three signaling pathways, including *NR4A1*(Fig. 1d). *NR4A1* encodes the Nur77 protein, which is significantly decreased in aged tissues, including liver, kidney and brain (Fig. 1e, Extended Data Fig. 1a), suggesting a potential role for Nur77 in the aging process.

To investigate the effects of Nur77 on aging, we established a natural aging model for wild type (WT) and *NR4A1*$^{-/-}$ mice (Extended Data Fig. 1b). In *NR4A1*$^{-/-}$ mice, impaired glucose tolerance and increased serum lipid contents, including triglycerides (TG) and total cholesterol (T-CHO), were evident by late adulthood (15 MO), significantly earlier than in WT mice (18 MO, Extended Data Fig. 1c-g). Deletion of *NR4A1* caused a rough decline of the median lifespan compared to WT mice (Fig. 1f). Moreover, dihydroethidium (DHE) staining and senescence-associated β-galactosidase (β-GAL) staining, which are indicative of accelerated ROS accumulation and organ aging, were observed in multiple organs of *NR4A1*$^{-/-}$ mice (15 MO) (Fig. 1g-h, Extended Data Fig. 1h). Similar to our *in vivo* results, analysis of *NR4A1*$^{-/-}$ mouse embryonic fibroblast (MEF) cells extracted from aged mice revealed elevated ROS and p53-dependent cell apoptosis under serum stimulation (Fig. 2a-d, Extended Data Fig. 2a).

Since mice lacking Nur77 showed elevated ROS levels, we tested the effect of Nur77 levels on the DNA damage response that is triggered by oxidative stress. Oxidative stress is an upstream pathogenic event that leads to cellular senescence and tissue aging. Indeed, Nur77 knockdown increased the H_2O_2-induced DNA damage response (Fig. 2d). By contrast, Nur77 overexpression decreased DNA damage response, as

indicated by the change in the phosphorylation state of ataxia-telangiectasia mutated (ATM) kinase at Ser1981 and checkpoint kinase 2 (Chk2) at Tyr68 (Fig. 2e).

We wondered if the effect of Nur77 on the DNA damage response is mediated through p53, a key factor in DNA damage repair pathway. Normally, the p53 protein has a short half-life due to rapid ubiquitylation by mouse double minute 2 (MDM2), which targets p53 for degradation by the proteasome[21]. In the presence of DNA damage, p53 is stabilized by phosphorylation on Ser20 via the protein kinase Chk2 (Extended Data Fig. 2b). To explore the requirement for p53, we transfected 1299 cells, a natural p53 deficiency cell line, with WT p53, S20A p53 (non-phosphorylation) or S20E p53 (phosphorylation mimic) (Extended Data Fig. 2c). We then tested the effect of Nur77 knockdown in each of the cell populations. We found Nur77 knockdown helped drive WT and S20E transfected cells into senescence, but not the S20A transfected cells (Extended Data Fig. 2c). We also found that Nur77 knockdown extended the half-life of p53 in cells treated with protein synthesis inhibitor cycloheximide (CHX), whereas simultaneously silencing Chk2 shortened the half-life of p53 (Extended Data Fig. 2d). Taken together, these results indicate that Nur77 knockdown aggravates the DNA damage response in a manner that is dependent on p53 stabilization.

The orphan nuclear receptor, Nur77 (also called TR3), shares common regulatory signaling pathways with SIRT1, including metabolic homeostasis, ROS removal and inflammatory response decline[19, 22–24]. We therefore hypothesized that Nur77 may contribute to SIRT1 protein homeostasis during aging. As Nur77 belongs to the nuclear receptor family, we first tested whether Nur77 is involved in the transcriptional regulation of SIRT1. The levels of *SIRT1* mRNA showed no obvious alteration in the presence or absence of Nur77 (Fig. 2f). However, Nur77 overexpression helped maintain SIRT1 protein homeostasis (Fig. 2g), whereas Nur77 knockdown reduced SIRT1 protein levels (Fig. 2g). These results suggest that the loss of SIRT1 protein in cellular senescence is dependent on aging-related Nur77 reduction.

SIRT1 deacetylates p53 in a NAD^+-dependent manner to inhibit the transcription activity of p53, which in turn modulates cellular senescence and apoptosis[5]. Moreover, SIRT1 alleviates the DNA damage response by removing ROS and accelerating DNA repair[25, 26]. We found that deletion of *NR4A1* resulted in disassociation of p53 from SIRT1 and promoted p53 interaction with CBP, a p53 acetyltransferase, which ultimately increased the acetylation of p53 at Lys382 (Fig. 2h,i, Extended Data Fig. 2e). Consistently, Nur77 knockdown augmented the p53 response to ROS, characterized by increased β-GAL staining, ROS accumulation and cell apoptosis (Fig. 2j-k, Extended Data Fig. 2e-g). As expected, SIRT1 overexpression rescued these effects (Fig. 2j-k, Extended Data Fig. 2e-g).

We next further clarified whether the Nur77 deficiency-induced p53 response is dependent on SIRT1 in H_2O_2-established senescent cells. In Nur77 overexpressing senescent cells, the repression of p53 by Nur77 was relieved upon knockdown of SIRT1 (Extended Data Fig. 3a). We also tested if the repression of p53 by Nur77 correlated with deacetylation of SIRT1. In *SIRT1*$^{-/-}$ HEK-293 cells, Nur77 overexpression attenuated DNA damage and apoptosis, as indicated by γh2AX and Bax when rescued with wild-type

(WT) SIRT1, but not when rescued with deacetylase inactive mutant SIRT1 (363HY, Extended Data Fig. 3b). This result suggests that the Nur77 regulation of p53 requires deacetylation of SIRT1 in senescent cells.

We then investigated the mechanism by which Nur77-stablizes SIRT1 protein homeostasis. Overexpressing Nur77 prolonged the half-life of SIRT1 in cells treated with CHX, whereas Nur77 knockdown significantly shortened the half-life (Fig. 3a). To test if Nur77-mediated SIRT1 protein homeostasis correlated with ubiquitin-proteasome system (UPS) degradation, we treated cells with the proteasome inhibitor MG132. Indeed, MG132 treatment restored SIRT1 protein in H_2O_2-induced senescent cells, including Nur77 knockdown senescent cells (Fig. 3b). We also tested whether the autophagy-lysosome pathway contributed to SIRT1 protein degradation in H_2O_2-induced senescent cells. Treatment with the autophagy inhibitor chloroquine (CQ) alone failed to rescue SIRT1 protein level in senescent cells, but when combined with MG132 could retore SIRT1 expression (Fig. 3b). This result indicates that SIRT1 is degraded through UPS during H_2O_2-induced cellular senescence and that Nur77 contributes to SIRT1 stability by inhibiting its degradation through UPS.

Along with SIRT1, Nur77 belongs to the group of nuclear and cytoplasmic shuttling proteins. However, we found no evidence of an interaction between Nur77 and SIRT1, suggesting Nur77 doesn't directly interact with SIRT1 to stabilize its protein homeostasis (Fig. 3c). We therefore investigated whether Nur77 regulates UPS degradation of SIRT1 through its E3 ligase. Previous studies showed that MDM2 is the main E3 ligase of SIRT1 during the DNA damage response[27]. Moreover, MDM2 is the second predicted E3 ligase for SIRT1 in UbiBrowser (Fig. 3d). Nur77 acts as a negative transcriptional factor of MDM2[28]. Indeed, we found Nur77 negatively regulated the expression of MDM2 at both the mRNA and protein levels (Fig. 3e-f). MDM2 overexpression also increased the ubiquitin labeling of SIRT1 under oxidative stress (Extended Data Fig. 3c). In response to a gradient concentration of H_2O_2 stimulation, the Nur77 and SIRT1 protein levels were significantly reduced, and the expression of MDM2, p53 and its acetylated form were elevated (Extended Data Fig. 3d). Therefore, we speculated that decreased Nur77 during oxidative stress-induced cellular senescence drives SIRT1 protein degradation and promotes the p53-mediated DNA damage response via the elevation of MDM2.

To determine if a decrease in Nur77 is a key initiating factor, we tested the response of the E3 ligase MDM2 to oxidative stress in the presence or absence of Nur77. Under H_2O_2 stimulation, Nur77 knockdown enhanced the specific recognition of SIRT1, but not p53, by MDM2 (Fig. 3g-h). This may be due to the DNA damage response resulting from Nur77 deficiency, which protects p53 against MDM2 recognition[29, 30]. Compared with the non-targeting control, the shorter half-life of SIRT1 protein conferred by Nur77 knockdown was rescued by silencing MDM2 (Fig. 4a). Moreover, Nur77 knockdown increased the ubiquitination of SIRT1 and decreased its expression, which could be rescued by silencing MDM2 (Fig. 4b-d). Consistently, overexpression of Nur77 helped protect SIRT1 from MDM2 recognition and ubiquitination (Fig. 4b-d). These results indicate that Nur77 enhances the stabilization of SIRT1 protein by suppressing MDM2 during oxidative stress-induced cellular senescence.

To gain functional insight, we investigated the effects of Nur77 deficiency on the kidney during the aging process and compared the changes in SIRT1, MDM2, and the p53-mediated signal in the presence or absence of Nur77. We found that the expression of SIRT1 protein in the kidney was significantly reduced with age, and observed an additional 39% decrease in the kidney with Nur77 deficiency compared to that in WT mice at late adulthood (15 MO) (Fig. 4e). Contrary to the decreased expression of SIRT1 that occurred with Nur77 deficiency at 15 MO, the expression of MDM2 protein was significantly increased (Fig. 4e, Extended Data Fig. 4c-d). Consequently, both an increase in the level of acetylated p53 and the activation of the apoptosis signal were noted (Fig. 4e). Consistent with *in vitro* studies, *SIRT1* mRNA levels were not altered in kidney, regardless of the presence or absence of Nur77, whereas the expression of *MDM2* mRNA increased with Nur77 deficiency (Fig. 4f-g). Notably, apoptosis and protease signals were enriched by differentially expressed genes, which included *MDM2*, screened from the *NR4A1*-deficient fawn hooded hypertensive rat model (Extended Data Fig. 4a-b). Meanwhile, p53-regulated senescence and apoptosis at late adulthood were augmented by Nur77 deficiency, as indicated by the elevation of senescence and pro-apoptosis proteins, including p53 and its phosphorylated form, p21 and Bax, and the reduction of the anti-apoptosis protein Bcl2 (Fig. 4h, Extended Data Fig. 4e-k). Therefore, Nur77 regulates the same biological mechanisms during the aging process as it does during oxidative stress-induced cellular senescence (Fig. 4i).

To evaluate the effect of Nur77 on kidney function, the creatinine (SCr) and urea nitrogen (BUN) levels in serum, urine volume (UV), the creatinine clearance rate (CCr), 24h urinary albumin (ALB) and the ratio of ALB to urinary creatinine (ACr) were analyzed (Fig. 5a-f). Beginning at late adulthood (15 MO), Nur77 deficiency resulted in higher SCr, BUN, ALB and ACr, whereas UV and CCr were remarkably decreased. These results underscore the finding that Nur77 deficiency aggravates the impairment of renal function during the aging process.

Morphological analysis at 15 MO revealed that deletion of Nur77 aggravated glomerular and podocyte injuries, as determined by Periodic Acid-Schiff (PAS) staining and Transmission Electron Microscope (TEM) scanning. Increased glomerular volume, thickening of Bowman's capsule, noticeable intestinal and periglomerular fibrosis were all observed in 15 MO kidney in which Nur77 was deleted (Fig. 5g-h, Extended Data Fig. 5a-c). Nur77 deletion in mice also increased DNA damage and podocyte loss (Fig. 5g,5i-j, Extended Data Fig. 5a, 5d-g). DNA damage was represented by the expressions of p53-binding protein 1 (53BP1), and the amount of podocyte apoptosis was determined by TdT mediated dUTP Nick End Labeling (TUNEL) and podocyte-associated proteins, Nephrin, respectively. These events in the kidney are associated with ROS accumulation with age. Nur77 deficiency aggravated ROS-induced cellular senescence and apoptosis in the kidney, and Nur77 in renal compartments demonstrates the dichotomous associations with aging nephropathy.

Discussion

Our findings reveal that loss of Nur77 with age augments the DNA damage response, cellular senescence and apoptosis, and accelerates the aging process in several mouse tissues. The classic longevity protein,

SIRT1, gradually degrades during the natural aging process, but the underlying regulatory mechanism has remained unclear. Our work reveals that Nur77 stabilizes the SIRT1 protein by reducing its degradation by the proteasome through negative transcriptional regulation of its E3 ligase MDM2. In addition, we confirmed the compelling role of Nur77 in protection against aging nephropathy via SIRT1. Still, these findings remain to be validated in other aging diseases in order to clarify the general role of Nur77-stabilized SIRT1 against aging.

We describe a heretofore unappreciated role of Nur77 in delaying the aging process. We find that Nur77 protein is reduced in multiple aged tissues and oxidase stress-induced senescent cells. We conclude that the downregulation of Nur77 in aged tissues may be associated with biological functions of organ aging and cellular senescence. Early functional studies have pointed to the critical role of Nur77 in negatively regulating the production of several senescence-associated secretory factors, including reactive oxygen, TNF-α, IL-1β and fatty acid[19, 22–24]. In this study, deletion of Nur77 resulted in shortened lifespan, ROS accumulation and the elevation of the senescent marker, β-galactosidase, in multiple tissues. Mice lacking Nur77 showed an earlier metabolic imbalance during the natural aging process. Nur77 knockdown aggravated the DNA damage response and cellular apoptosis upon senescence-related stimulation. Therefore, Nur77 deficiency that occurs with age seems to be a driving factor for the accelerated aging process.

SIRT1 is involved in the regulation of various important senescence-related biological processes, including the inhibition of inflammation, DNA damage and cellular apoptosis[4–6]. The aging process usually presents with chronic p53 activation[31, 32]. SIRT1 represses the activated and stabilized form of p53[25, 26]. Recent studies have shown no obvious alteration of SIRT1 mRNA in DNA damage-induced senescence[33]. The reduction of SIRT1 during aging may be mainly attributed to increased protein degradation. Nur77 and SIRT1 share many similarities in the regulation of aging-related biological pathways. Our findings suggest Nur77 stabilizes the homeostasis of SIRT1 protein against UPS degradation indirectly, through the regulation of the E3 ligase of SIRT1. In the DNA damage response, the main E3 ligase of SIRT1 has been confirmed to be MDM2, which is also the classic E3 ligase of p53[21, 27]. Nur77 suppresses the expression of MDM2 at both the transcriptional and post-transcriptional levels[28]. Our work suggests that Nur77 deficiency with age leads to the selective degradation of SIRT1 protein by MDM2-mediated UPS activation under oxidative stress, whereas increased phosphorylation of p53 on Ser20 by Chk2 protects it from recognition by MDM2. These events constitute positive feedback for the acceleration of the aging process: reduction of Nur77 by oxidative stress breaks down the homeostasis of SIRT1 protein through MDM2, resulting in cellular senescence and apoptosis, and an increase in reactive oxygen production, which in turn further decrease the expression of Nur77 and accelerate the aging process.

SIRT1 is widely expressed in tubular cells and podocytes of kidney[34]. Podocytes maintain the glomerular filtration barrier, and initial glomerular injury affects podocytes as important target cells for progression of aging nephropathy[35]. Podocyte-specific deletion of SIRT1 results in ROS accumulation, inflammatory

response and podocyte loss in kidney[36, 37]. We further illustrated the effects of Nur77 in renal aging, which may be representative of the general role of Nur77 in aging diseases. Our results reveal that the expression of Nur77 in kidney decrease gradually during the natural aging process. SIRT1 is significantly reduced in the kidneys under Nur77 deficiency, corresponding with the activation of senescent and apoptosis signals. Nur77 deficiency aggravates aging-related morphological changes and functional damage of the kidney. Therefore, Nur77 may be a new therapeutic target to combat aging related nephropathy.

Collectively, our study shows for the first time that Nur77 is an important contributor to the effort to combat the aging process. Nur77 is also an important upstream regulator for the maintenance of SIRT1 protein homeostasis during the aging process. Preventing Nur77 reduction with age by pharmacological targeting at late adulthood may be a novel approach for the treatment of aging diseases.

Materials And Methods

Mouse Experiments

All animal experiments were approved by the Animal Ethics Committee of China Medical University (CMU2019277). Wild type (WT) and *NR4A1*-targeted mutant (No: 006187; *NR4A1*$^{-/-}$) mice with a C57BL/6J background were purchased from The Jackson Laboratory (Bar Harbor, ME, USA). *NR4A1*-targeted mutant mice were produced with a neomycin cassette introduced to exon 2 of the mouse Nur77 to block the transcription of both the DNA binding domain (DBD) and ligand-binding (LBD) domain[38]. All mice were housed in a temperature and climate-controlled barrier system (23 ± 2°C and 45–60% relative humidity, 12 h cycle of light and darkness), and fed regular rodent chow. Naturally aging mice were divided into 4 groups for analysis (5-, 8-, 15-, 18-month-old). Young serum (YS) and old serum (OS) were extracted from 5- and 18-month-old mice, respectively. The number of surviving mice for WT (n=10) and *NR4A1*$^{-/-}$ (n=10) was recorded every month for 24 months. Then the mice were divided into four groups for analysis: 5-month-old mice (WT-5 MO; n=6) and (*NR4A1*$^{-/-}$-15 MO; n=6) groups; 15-month-old mice (WT-15 MO; n=6) and (*NR4A1*$^{-/-}$-15 MO; n=6) groups. Urine samples were collected by placing each mouse in an individual metabolic cage (Tecniplast, Gazzada, Italy) for 24 h. Oral glucose tolerance test (OGTT) was performed at 0, 30, 60, 90, 120 min using an Accu-Chek meter (Roche; MO, USA). Fasting blood glucose (FBG), total cholesterol (CHOL), triglyceride (TAG), creatine (Cr) and urea nitrogen (BUN) were determined as per the test kit manufacturer's instructions (Jiancheng, Nanjing, China).

Histological Staining for Tissues and Analysis

For H&E, Sirius red, Masson's trichrome and Periodic acid–Schiff (PAS) staining, tissues were isolated and fixed overnight at 4°C, and treated with 30% sucrose for cryoprotection. Sections of kidney were dewaxed with xylene and a series of descending ethanol gradients. Then sections were stained with Mayer's H&E (Jiancheng) or Sirius Red F3B and a saturated aqueous solution of picric acid (Solarbio, beijing, China), Masson (Jiancheng) or PAS kit (Solarbio), and observed with a Nikon Eclipse Ni-U

microscope. For immunohistochemistry (IHC), paraffin sections were stained with anti-Nephrin (Abcam, Cambridge, UK), assessed by light microscopy and quantified using ImageJ (Wayne Rasband, US National Institutes of Health, Bethesda, MD, USA). For β-GAL, TUNEL and immunofluorescence staining, frozen tissue slices were stained with a β-GAL kit (Beyotime, Biotechnology, Shanghai, China), TUNEL kit (Beyotime), or anti-53BP1 (NOVUS, Abingdon, UK), respectively, photographed using an Olympus IX-71 fluorescence microscope and quantified using ImageJ. For DHE staining, 24 h before killing, mice received a 200 μL intravenous injection of dihydroethidium kit (Sigma-Aldrich, St Louis, MI, USA) at 25 mg/kg, and frozen tissue slices were photographed using an Olympus IX-71 fluorescence microscope and quantified using ImageJ.

Transmission Electron Microscopy (TEM)

For electron microscopy, sample handling and detection were performed by Wuhan servicebio technology. Tissues were collected and fixed with 2.5% glutaraldehyde at 4°C. Sections were washed with PBS and fixed in 1% osmium tetroxide at room temperature for 2 h. Specimens were then dehydrated using a series of ascending ethanol gradients and 100% acetone in series. After dehydration, the sections were embedded in Pon 812 resin overnight at 37°C using acetone as a transitional solvent. The ultra-thin sections were stained with 2% saturated uranyl acetate and lead citrate. The glomerular Basement Membrane (GBM) thickness, foot process width and the number of foot processes per μm of GBM, TEM images were analyzed using ImageJ.

Glutathione Peroxidase (GSH-PX) and Superoxide dismutase (SOD) detection

Tissues were washed with PBS and homogenized with cold Tris–HCl buffer (pH 7.4) to obtain 10% homogenate. GSH-PX and SOD in serum and kidney tissues were measured kinetically according to the method of the corresponding enzymatic assays (Jiancheng), and quantified using an automatic analyzer.

RNA-Sequencing Analysis

RNA sequencing data were downloaded and referenced to the Gene Expression Omnibus under accession number (GSE54714, GSE6591, GSE8150, GSE25905). A log fold change (log_2FC) > 1.5 and an adjusted *p*-value < 0.05 were set as the thresholds for the identification of differentially expressed genes. Bioinformatic analyses using the Metascape pathway analysis[39] and Ingenuity Pathways Analysis[40] were carried out to determine molecular functions and upstream signaling pathways.

Cell Culture and Treatments

Mouse embryonic fibroblasts (MEFs) were derived from E14.5 embryos from *NR4A1*$^{+/-}$ C57BL/6J mice, and cultured in DMEM medium with 15% FBS (Gibco, Carlsbad, CA, USA), 100 units/mL penicillin, and 10 mg/mL streptomycin. Then they were treated with serum from aged mice (OS) or young mice (YS) as a normal control for 24 h. Human embryonic kidney (HEK) 293 cell lines were obtained from the American

Type Culture Collection and cultured in DMEM medium with 10% FBS. H1299 cells are a p53-deficient cell line obtained from the American Type Culture Collection and cultured in 1640 medium with 10% FBS. For DNA damage-triggered senescence, 293 cells were treated with 500 μM H_2O_2 for 4 h. Transfection was performed using Lipo3000 (Thermo Fisher Scientific, Waltham, MA, USA).

Plasmids

Nur77 overexpression and shRNA lentiviruses were purchased from GeneChem (Shanghai, China). The HA-tagged SIRT1 *WT* or deacetylase-inactive mutant (*363HY*) plasmids were constructed and described previously[41]. *CBP*, *p300*, *GCN5* and *PCAF* plasmids were constructed and described previously[42]. *SIRT1*, *MDM2* and *CBP* siRNA were purchased from RiboBio. *GFP-MDM2*, *Ub* and Site-directed mutagenesis (*WT*, *S20A*, *S20E*) of *Flag-p53* plasmids was performed using QuikChange XL (Stratagene) and confirmed by sequencing. *SIRT1*$^{-/-}$ and *Chk2*$^{-/-}$ Cas9 HEK-293 cells were constructed and provided by Wenyu Zhang[43].

Co-immunoprecipitation (Co-IP) and western blot analysis

Co-IP and western blot analysis were performed as previously described[44]. The different primary antibodies used are indicated in Supplementary Table 1.

Real-Time PCR

RNA was isolated from podocytes using the RNeasy Plus Mini Kit (Qiagen, Hilden, Germany). Copy DNA was prepared using a PrimeScript™ RT reagent Kit (TaKaRa, Kusatsu, Japan) followed by quantitative Real-Time PCR using SYBR Green (TaKaRa). Relative quantitation was carried out using $2^{-\Delta\Delta CT}$. RT-PCR primers are listed in Supplementary Table 2.

Protein degradation assays

For the determination of the half-life of proteins, cells were pretreated with 100 μM H_2O_2 for 6 h, then incubated with 100 μg/mL cycloheximide (CHX; APExBIO, Houston, TX, USA) for 0, 3, 6 and 9 h (SIRT1) or 0, 30 ,60 and 90 min (p53), followed by sample harvesting and western blot analysis. To determine whether SIRT1 expression is affected by proteasome-dependent proteolysis, cells were treated with 50 μM MG132 (Selleck Chemicals, Houston, TX, USA) for 4 h, with/without 20 μM chloroquine (CQ; Sigma-Aldrich) for 10 h. For ubiquitination assays, cells were co-transfected with HA-SIRT1, Ubiquitin (Ub) and GFP-MDM2 plasmids. After 30 h post-transfection, cells were harvested followed by co-immunoprecipitation (Co-IP) analysis.

Flow Cytometry

Apoptosis assessments were made based on allophycocyanin (APC) Annexin V and propidium iodide (PI) staining (Thermo Fisher). Cells were harvested followed by staining with APC Annexin V and PI as per the manufacturer's instructions. ROS was determined by a fluorometric intracellular ROS Kit (Sigma-Aldrich) according to the manufacturer's instructions. After stimulation, cells were then incubated in Hank's

balanced salt solution containing 5 mM 2',7'-Dichlorodihydrofluorescein diacetate (DCFH-DA) for 1 h, and analyzed by flow cytometry using FACS caliber (Becton Dickinson, Franklin Lakes, NJ, USA).

Cell Counting Kit-8 (CCK8)

After transfection and stimulation, cell viability was counted using the CCK8 kit. The fluorescence intensity in each well was then measured at 450 nm.

Statistical analyses

Data ($n > 6$) are expressed as mean ± standard error (SE). Data ($n \leq 6$) are expressed as mean ± standard deviation (SD). Unpaired two-tailed Student's t-test and Mann-Whitney test were used for comparison between two groups. One-way ANOVA coupled with Tukey's multiple comparison test or two-way ANOVA coupled with Sidak's multiple comparisons tests were used for comparisons over two groups. $p < 0.05$ was considered significant. The number of repetitions for each experiment is indicated in the figure legends.

Data availability

RNA sequencing data were referenced to the Gene Expression Omnibus under accession number (GSE54714, GSE6591, GSE8150, GSE25905). All other data supporting the findings of this study are available from the corresponding author upon reasonable request.

Declarations

Competing interests

The authors have declared that no conflict of interest exists.

Author contributions

L.C. and D.W. designed the experiments and revised the manuscript. Y.Y. performed most of the experiments and wrote the manuscript. X.S. performed the mouse experiments and helped with manuscript writing. G.M., L.Z. F.C. Y.X. and T.L. helped with primary MEF extraction and cell culture. X.W. and H.T. helped with conducting flow cytometry. X.W., D.L. and F.Y. were responsible for bioinformatic analysis. All authors discussed the results and reviewed the manuscript.

Acknowledgement

This study was supported by the National Key R&D Program of China (2016YFC1302400), the Ministry of Education Innovation Team Development plan (IRT_17R107), the National Science Foundation of China

(82000827), Liaoning Provincial Doctoral Fund (2020-BS-087) and the Talent Project for Revitalizing Liaoning, People's Republic of China (XLYC1902013).

Abbreviations

ACR
the ratio of ALB to urinary creatinine; ALB:urinary albumin; AUC:area under the curve; BUN:blood urea nitrogen; BW:Body weights; CCr:creatinine clearance rate; CHOL:total cholesterol; CHX:cycloheximide; CQ:chloroquine; DCFH:dichlorodihydrofluorescein diacetate; DHE:dihydroethidium; DMSO:dimethyl sulfoxide; FBG:fasting blood glucose; GSH-PX:glutathione peroxidase; IB:immunoblot; IHC:immunohistochemistry; IP:immunoprecipitation; MO:month-old; ROS:reactive oxygen species; SCr:serum creatinine; SOD:superoxide dismutase; TAG:triglyceride; TUNEL:terminal deoxynucleotidyl transferase dUTP nick end label; Ub:ubiquitin; UV:urine volume; WT:wild-type

References

1. Lopez-Otin, C., Blasco, M.A., Partridge, L., Serrano, M. & Kroemer, G. The hallmarks of aging. *Cell* **153**, 1194–1217 (2013).
2. Imai, S. & Guarente, L. NAD + and sirtuins in aging and disease. *Trends Cell Biol* **24**, 464–471 (2014).
3. Mouchiroud, L. *et al.* The NAD(+)/Sirtuin Pathway Modulates Longevity through Activation of Mitochondrial UPR and FOXO Signaling. *Cell* **154**, 430–441 (2013).
4. Wellman, A.S. *et al.* Intestinal Epithelial Sirtuin 1 Regulates Intestinal Inflammation During Aging in Mice by Altering the Intestinal Microbiota. *Gastroenterology* **153**, 772–786 (2017).
5. Bi, X. *et al.* Inhibition of nucleolar stress response by Sirt1: A potential mechanism of acetylation-independent regulation of p53 accumulation. *Aging Cell* **18**, e12900 (2019).
6. Gomes, A.P. *et al.* Declining NAD(+) induces a pseudohypoxic state disrupting nuclear-mitochondrial communication during aging. *Cell* **155**, 1624–1638 (2013).
7. Meng, F. *et al.* Synergy between SIRT1 and SIRT6 helps recognize DNA breaks and potentiates the DNA damage response and repair in humans and mice. *Elife* **9** (2020).
8. Yoshino, J., Mills, K.F., Yoon, M.J. & Imai, S. Nicotinamide mononucleotide, a key NAD(+) intermediate, treats the pathophysiology of diet- and age-induced diabetes in mice. *Cell Metab* **14**, 528–536 (2011).
9. Prola, A. *et al.* SIRT1 protects the heart from ER stress-induced cell death through eIF2alpha deacetylation. *Cell Death Differ* **24**, 343–356 (2017).
10. Donato, A.J. *et al.* SIRT-1 and vascular endothelial dysfunction with ageing in mice and humans. *J Physiol* **589**, 4545–4554 (2011).
11. Szilard, L. On the Nature of the Aging Process. *Proc Natl Acad Sci U S A* **45**, 30–45 (1959).
12. Li, C. *et al.* Mitochondrial DNA stress triggers autophagy-dependent ferroptotic death. *Autophagy* **17**, 948–960 (2021).

13. Butin-Israeli, V. *et al.* Neutrophil-induced genomic instability impedes resolution of inflammation and wound healing. *J Clin Invest* **129**, 712–726 (2019).
14. Nieborowska-Skorska, M. *et al.* Rac2-MRC-cIII-generated ROS cause genomic instability in chronic myeloid leukemia stem cells and primitive progenitors. *Blood* **119**, 4253–4263 (2012).
15. Tang, Y. *et al.* Resveratrol reduces vascular cell senescence through attenuation of oxidative stress by SIRT1/NADPH oxidase-dependent mechanisms. *J Nutr Biochem* **23**, 1410–1416 (2012).
16. Kwon, S. *et al.* Obesity and aging diminish sirtuin 1 (SIRT1)-mediated deacetylation of SIRT3, leading to hyperacetylation and decreased activity and stability of SIRT3. *J Biol Chem* **292**, 17312–17323 (2017).
17. Li, L. *et al.* Impeding the interaction between Nur77 and p38 reduces LPS-induced inflammation. *Nat Chem Biol* **11**, 339–346 (2015).
18. Bian, X.L. *et al.* Nur77 suppresses hepatocellular carcinoma via switching glucose metabolism toward gluconeogenesis through attenuating phosphoenolpyruvate carboxykinase sumoylation. *Nat Commun* **8**, 14420 (2017).
19. Li, X.X. *et al.* Nuclear Receptor Nur77 Facilitates Melanoma Cell Survival under Metabolic Stress by Protecting Fatty Acid Oxidation. *Mol Cell* **69**, 480–492 e487 (2018).
20. Koenis, D.S. *et al.* Nuclear Receptor Nur77 Limits the Macrophage Inflammatory Response through Transcriptional Reprogramming of Mitochondrial Metabolism. *Cell Rep* **24**, 2127–2140 e2127 (2018).
21. Haupt, Y., Maya, R., Kazaz, A. & Oren, M. Mdm2 promotes the rapid degradation of p53. *Nature* **387**, 296–299 (1997).
22. Hedrick, E., Mohankumar, K., Lacey, A. & Safe, S. Inhibition of NR4A1 Promotes ROS Accumulation and IL24-Dependent Growth Arrest in Rhabdomyosarcoma. *Mol Cancer Res* **17**, 2221–2232 (2019).
23. Yang, P.B. *et al.* Blocking PPARgamma interaction facilitates Nur77 interdiction of fatty acid uptake and suppresses breast cancer progression. *Proc Natl Acad Sci U S A* **117**, 27412–27422 (2020).
24. Hu, M. *et al.* Celastrol-Induced Nur77 Interaction with TRAF2 Alleviates Inflammation by Promoting Mitochondrial Ubiquitination and Autophagy. *Mol Cell* **66**, 141–153 e146 (2017).
25. Kwon, J., Lee, S., Kim, Y.N. & Lee, I.H. Deacetylation of CHK2 by SIRT1 protects cells from oxidative stress-dependent DNA damage response. *Exp Mol Med* **51**, 1–9 (2019).
26. Liu, T. *et al.* SIRT1 reverses senescence via enhancing autophagy and attenuates oxidative stress-induced apoptosis through promoting p53 degradation. *Int J Biol Macromol* **117**, 225–234 (2018).
27. Peng, L. *et al.* Ubiquitinated sirtuin 1 (SIRT1) function is modulated during DNA damage-induced cell death and survival. *J Biol Chem* **290**, 8904–8912 (2015).
28. Zhao, B.X. *et al.* p53 mediates the negative regulation of MDM2 by orphan receptor TR3. *EMBO J* **25**, 5703–5715 (2006).
29. Chehab, N.H., Malikzay, A., Appel, M. & Halazonetis, T.D. Chk2/hCds1 functions as a DNA damage checkpoint in G(1) by stabilizing p53. *Genes Dev* **14**, 278–288 (2000).

30. Bernardi, R. *et al.* PML regulates p53 stability by sequestering Mdm2 to the nucleolus. *Nat Cell Biol* **6**, 665–672 (2004).
31. Hirao, A. *et al.* DNA damage-induced activation of p53 by the checkpoint kinase Chk2. *Science* **287**, 1824–1827 (2000).
32. Zhu, L.Y. *et al.* Aging Induced p53/p21 in Genioglossus Muscle Stem Cells and Enhanced Upper Airway Injury. *Stem Cells Int* 2020, 8412598 (2020).
33. Xu, C. *et al.* SIRT1 is downregulated by autophagy in senescence and ageing. *Nat Cell Biol* **22**, 1170–1179 (2020).
34. Zhong, Y., Lee, K. & He, J.C. SIRT1 Is a Potential Drug Target for Treatment of Diabetic Kidney Disease. *Front Endocrinol (Lausanne)* **9**, 624 (2018).
35. Nagata, M. Podocyte injury and its consequences. *Kidney Int* **89**, 1221–1230 (2016).
36. Chuang, P.Y. *et al.* Reduction in podocyte SIRT1 accelerates kidney injury in aging mice. *Am J Physiol Renal Physiol* **313**, F621-F628 (2017).
37. Hong, Q. *et al.* Increased podocyte Sirtuin-1 function attenuates diabetic kidney injury. *Kidney Int* **93**, 1330–1343 (2018).
38. Lee, S.L. *et al.* Unimpaired thymic and peripheral T cell death in mice lacking the nuclear receptor NGFI-B (Nur77). *Science* **269**, 532–535 (1995).
39. Tripathi, S. *et al.* Meta- and Orthogonal Integration of Influenza "OMICs" Data Defines a Role for UBR4 in Virus Budding. *Cell Host Microbe* **18**, 723–735 (2015).
40. Kramer, A., Green, J., Pollard, J., Jr. & Tugendreich, S. Causal analysis approaches in Ingenuity Pathway Analysis. *Bioinformatics* **30**, 523–530 (2014).
41. Wang, C. *et al.* Interactions between E2F1 and SirT1 regulate apoptotic response to DNA damage. *Nat Cell Biol* **8**, 1025–1031 (2006).
42. Yi, F. *et al.* The deacetylation-phosphorylation regulation of SIRT2-SMC1A axis as a mechanism of antimitotic catastrophe in early tumorigenesis. *Sci Adv* **7** (2021).
43. Zhang, W. *et al.* SIRT1 modulates cell cycle progression by regulating CHK2 acetylation-phosphorylation. *Cell Death Differ* **27**, 482–496 (2020).
44. Fu, Y. *et al.* Elevation of JAML Promotes Diabetic Kidney Disease by Modulating Podocyte Lipid Metabolism. *Cell Metab* **32**, 1052–1062 e1058 (2020).

Figures

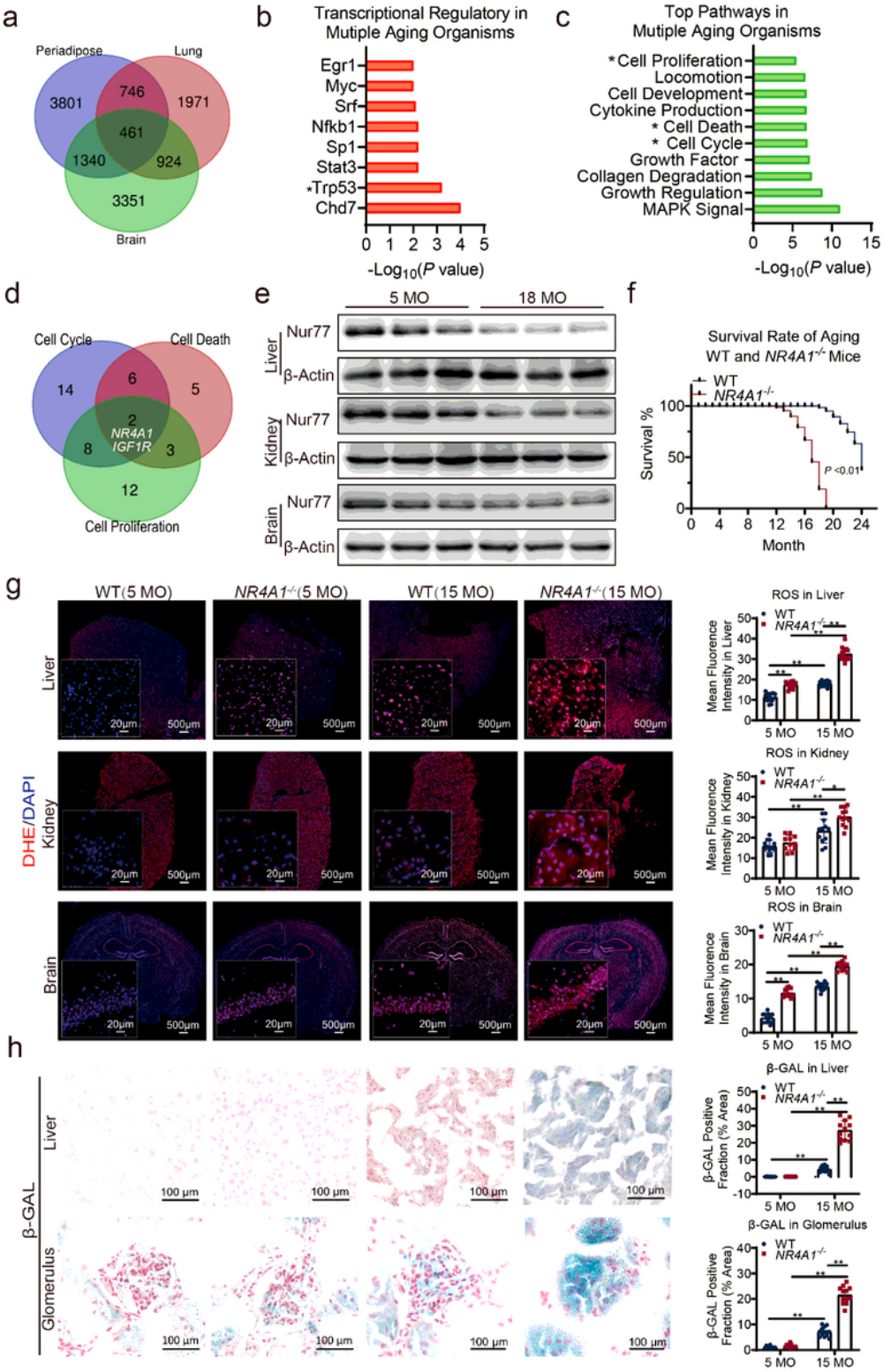

Figure 1

Deletion of Nur77 augments the aging process. a. Venn diagram showing the intersection of differentially expressed genes in peri-adipose, lung and brain of three naturally aging mice models. b. The top transcription factors for the regulation of co- differentially expressed genes in multiple aging organisms identified by TRRUST. c. The top pathways for the regulation of co- differentially expressed genes in multiple aging organisms identified by Metascape. D. Venn diagram showing the intersection of

differentially expressed genes in cell cycle, cell death and cell proliferation in multiple aging organisms. e. Nur77 expression in liver, kidney and brain of aged and adult mice as determined by western blot. n=2 independent experiments. f. The comparison of survival rates of aging WT and NR4A1-/- mice. g. The dihydroethidium (DHE) staining of liver, kidney and brain. Scale bars are indicated for the figure and insets. h. β- galactosidase staining of liver and kidney. Scale bar: 100 μm.

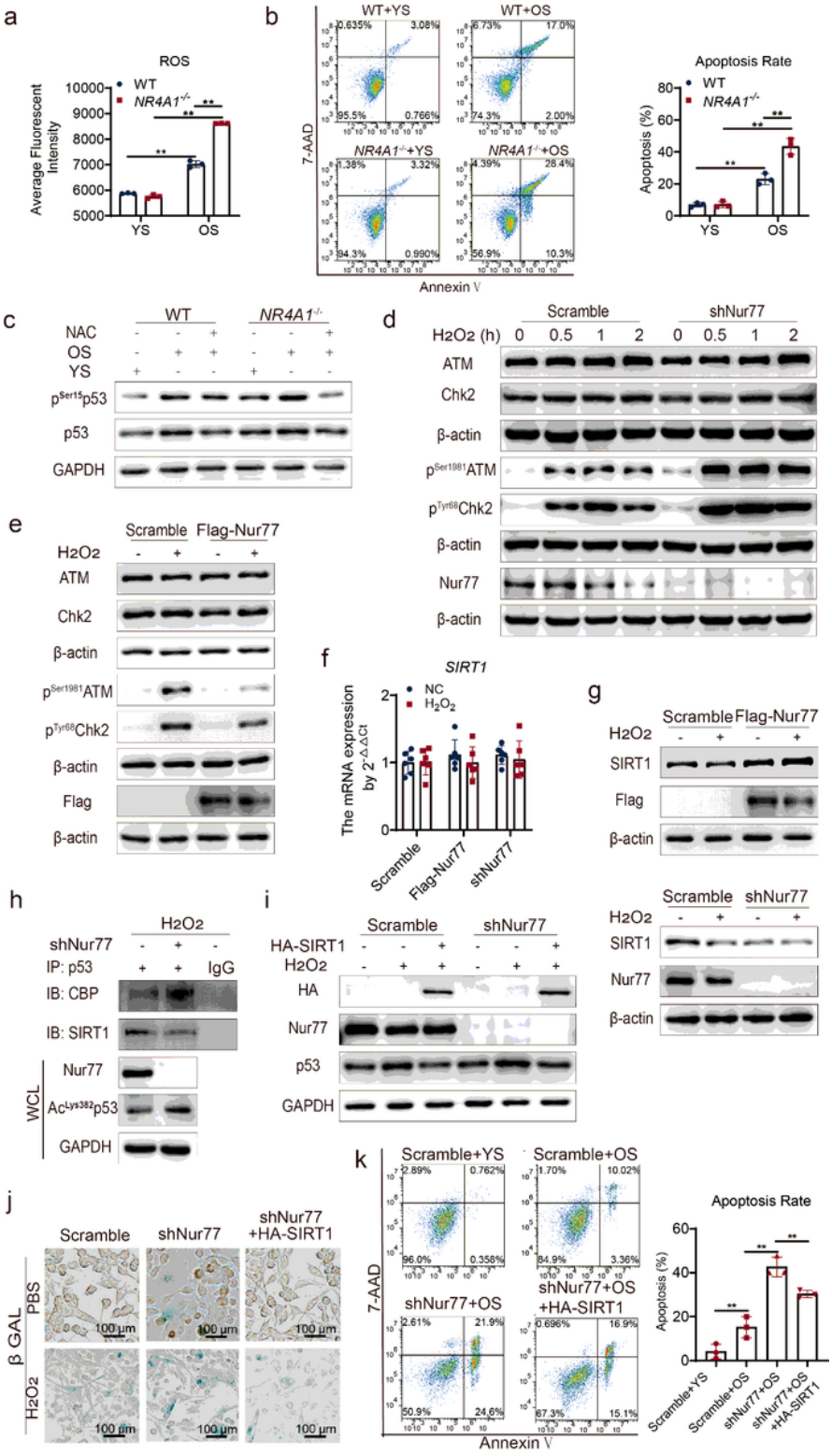

Figure 2

Nur77 attenuates oxidative stress-triggered cell senescence by enhancing the homeostasis of SIRT1. a. The reactive oxygen species (ROS) in WT and NR4A1-/- MEF cells under serum treatment from aged mice (OS) or young mice (YS) as determined by flow cytometry. n=3 independent experiments. b. The apoptosis rate in WT and NR4A1-/- MEF cells under OS or YS serum treatment as determined by flow cytometry. n=3 independent experiments. c. Western blot analysis of p53 and pSer15p53 expression levels in WT and NR4A1-/- MEF cells under OS or YS serum treatment with N-Acetyl-L-cysteine (NAC). n=2 independent experiments. d. Western blot analysis of ATM, pSer1981ATM, Chk2, pTyr68Chk2 expression levels in cells under H2O2 stimulation with or without Nur77 knockdown. n=3 independent experiments. e. Western blot analysis of ATM, pSer1981ATM, Chk2, pTyr68Chk2 expression levels in cells under H2O2 stimulation with or without Nur77 overexpression. n=3 independent experiments. f. RT-PCR analysis of SIRT1 mRNA expression in the presence or absence of Nur77. n=6 independent experiments. g. Western blot analysis of SIRT1 expression in the presence or absence of Nur77. n=3 independent experiments. h. Co-IP analysis of the interaction between p53 and SIRT1 or CBP with or without Nur77 knockdown. n=2 independent experiments. i. Analysis of the activation of p53 in cells with or without Nur77 knockdown in the presence of SIRT1 overexpression. n=2 independent experiments. j. β- galactosidase staining of HEK-293 cells under the indicated conditions. Scale bar: 100 μm. k. The apoptosis rate of HEK-293 cells under the indicated conditions. n=3 independent experiments.

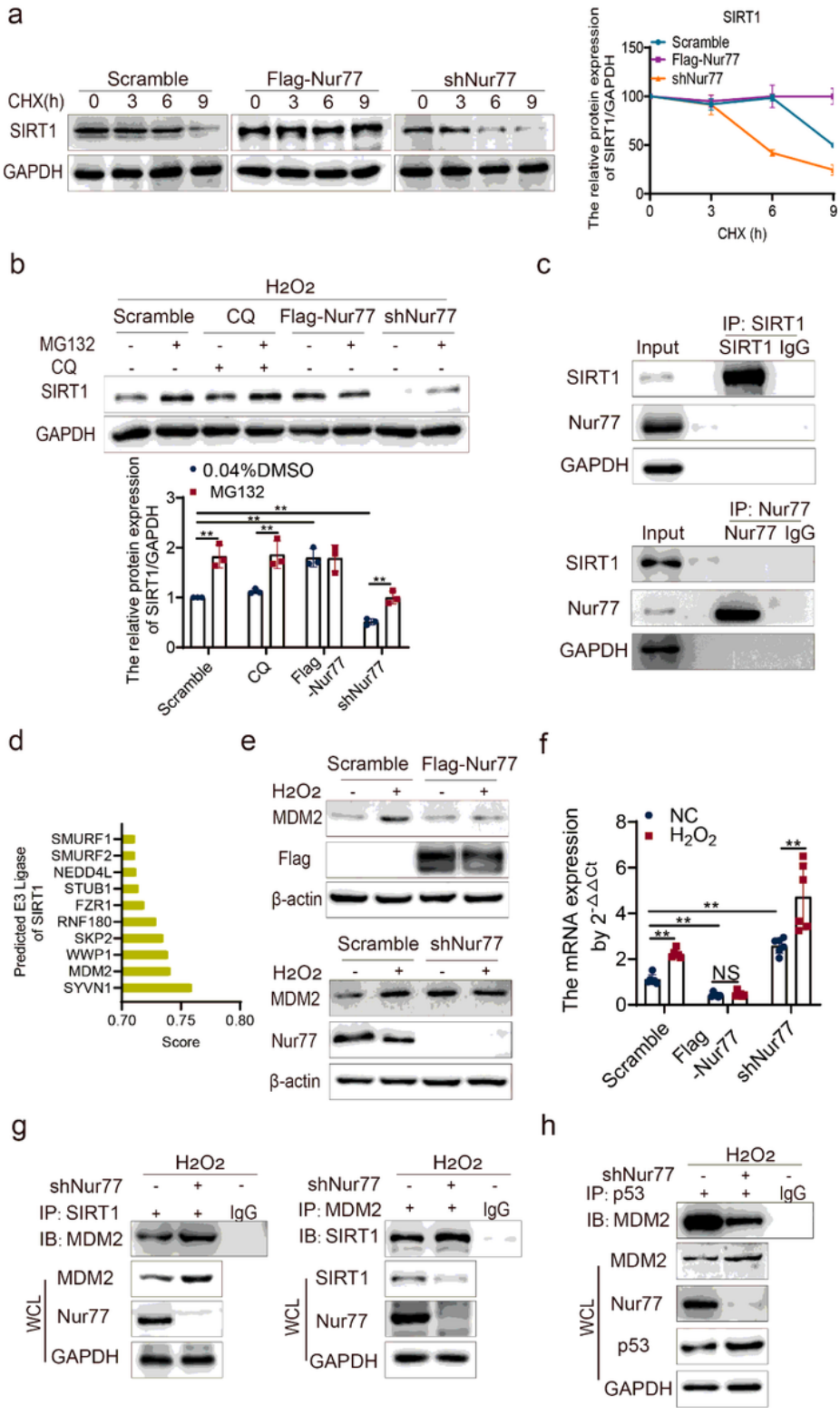

Figure 3

Nur77 stabilizes the homeostasis of SIRT1 via negative transcriptional regulation of MDM2. a. SIRT1 expression in the presence or absence of Nur77 and 100 μg/mL CHX. n=3 independent experiments. b. SIRT1 expression in the presence or absence of Nur77 and 50 μM MG132 for 4 h, or 20 μM CQ for 10 h. n=3 independent experiments. c. Co-IP analysis of the interaction between Nur77 and SIRT1. n=2 independent experiments. d. The E3 ligase prediction for SIRT1 by the UbiBrowser database. e. MDM2

expression in the presence or absence of Nur77. n=3 independent experiments. f. RT-PCR analysis of MDM2 mRNA expression in the presence or absence of Nur77. n=6 independent experiments. g. Co-IP analysis of the interaction between MDM2 and SIRT1 upon Nur77 knockdown. n=2 independent experiments. h. Co-IP analysis of the interaction between MDM2 and p53 upon Nur77 knockdown. n=2 independent experiments.

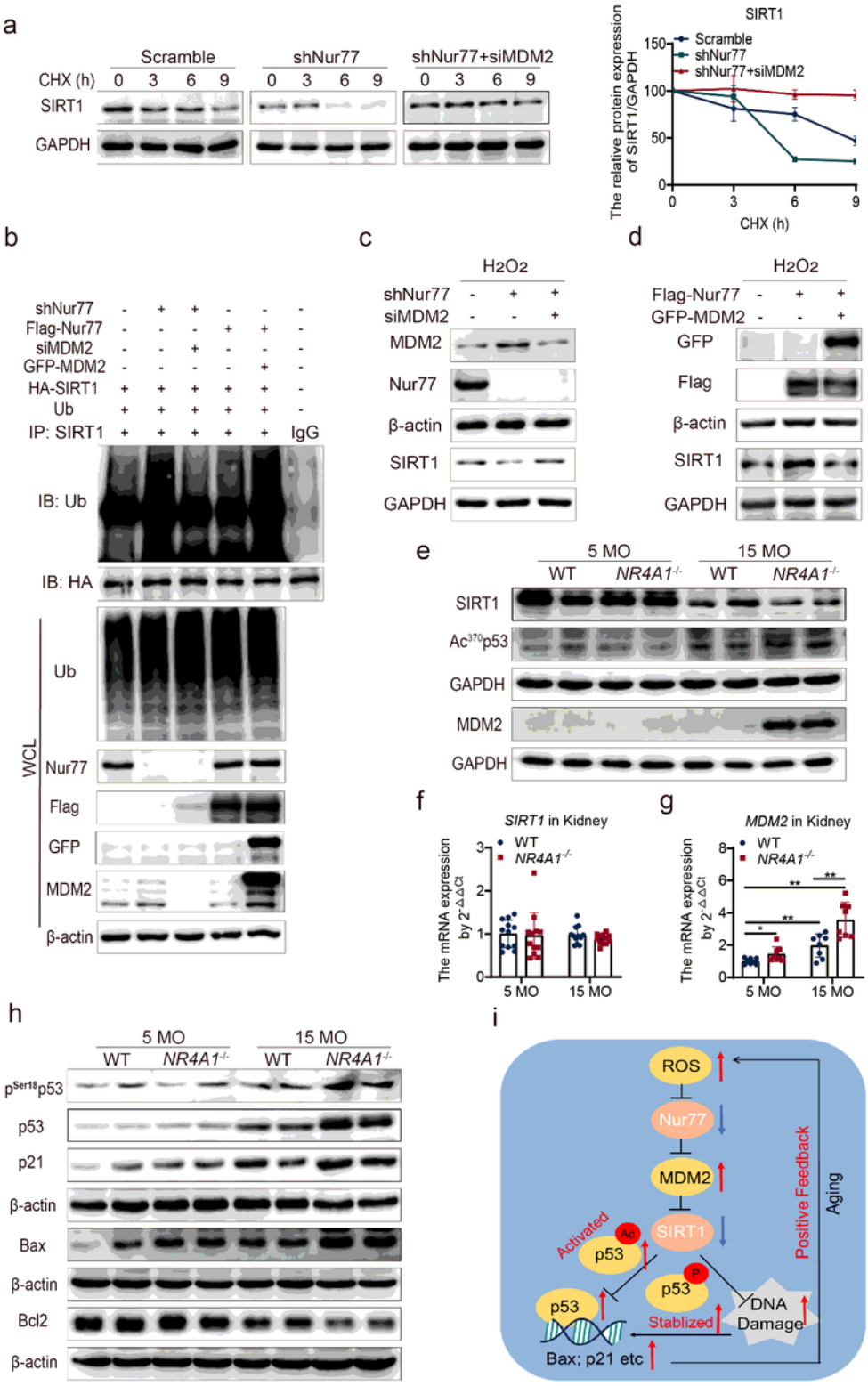

Figure 4

Nur77 deficiency augments MDM2-mediated SIRT1 degradation, senescence and apoptosis. a. Effect of simultaneous knockdown of Nur77 and MDM2 on SIRT1 expression in cells treated with 100 μg/mL CHX. n=3 independent experiments. b. Analysis of ubiquitination of SIRT1 in the presence or absence of Nur77 or MDM2. n=2 independent experiments. c-d. SIRT1 expression in the presence or absence of Nur77 or MDM2. n=2 independent experiments. e. SIRT1, MDM2 and Ac370p53 expression levels in kidney tissue. n=2 independent experiments. f. SIRT1 mRNA expression in kidney tissue. n=6 independent experiments. g. MDM2 mRNA expression in kidney tissue. n=6 independent experiments. h. p53, Ser18p53, p21, Bax and Bcl2 expression levels in kidney tissue. n=2 independent experiments. i. The positive feedback initiated by aging-related Nur77 deficiency accelerates the degradation of SIRT1 and impairs organism homeostasis.

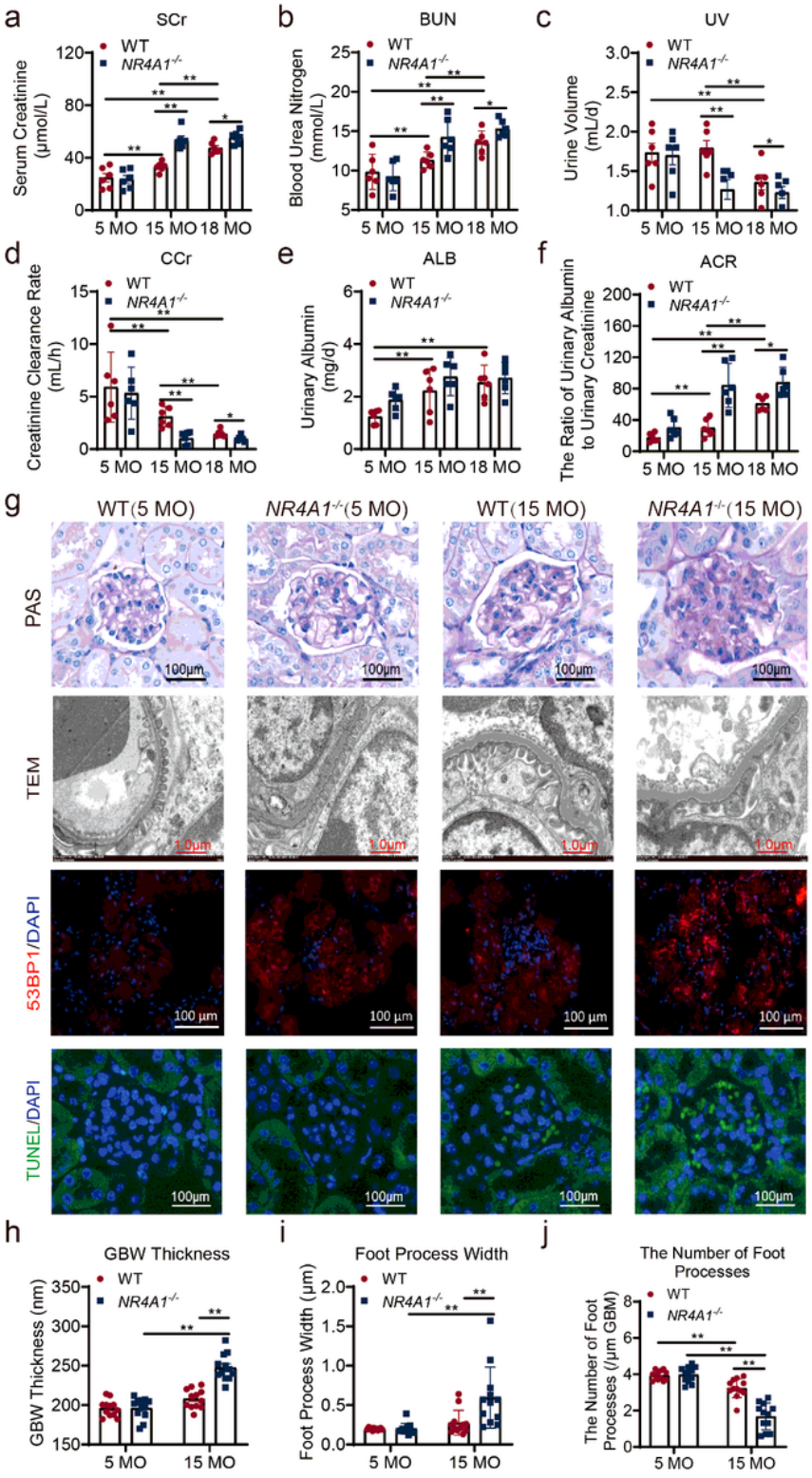

Figure 5

Nur77 deficiency aggravates functional and morphological injury of kidneys during the aging process. Comparison of kidney function-related parameters relating to serum creatinine (SCr, a), blood urea nitrogen (BUN, b), urine volume (UV, c), creatinine clearance rate (CCr, d), urinary albumin (ALB, e) and the ratio of ALB to urinary creatinine (ACR, f) between WT and NR4A1-/- mice. CCr = UV×UCr/(SCr×24×BW). g. Morphological examination of glomerular by Periodic acid–Schiff (PAS), Transmission electron

microscopy (TEM), immunofluorescence of 53BP1 and TdT mediated dUTP Nick End Labeling (TUNEL). Scale bars are indicated. h-j. The analyses of the glomerular Basement Membrane (GBM) thickness, foot process width and the number of foot processes per μm of GBM. 6 glomeruli per mouse were analyzed, n = 2 mice per group.

Supplementary Files

This is a list of supplementary files associated with this preprint. Click to download.

- Supplymentarydata.pdf